Published online 22 May 2007

Nucleic Acids Research, 2007, Vol. 35, No. 11 ***3797–3809***
doi:10.1093/nar/gkm158

Aprataxin, causative gene product for EAOH/AOA1, repairs DNA single-strand breaks with damaged 3′-phosphate and 3′-phosphoglycolate ends

Tetsuya Takahashi[1], Masayoshi Tada[1], Shuichi Igarashi[1,2], Akihide Koyama[1], Hidetoshi Date[4], Akio Yokoseki[1], Atsushi Shiga[1], Yutaka Yoshida[3], Shoji Tsuji[4], Masatoyo Nishizawa[1] and Osamu Onodera[2,*]

[1]Department of Neurology, Clinical Neuroscience Branch, [2]Department of Molecular Neuroscience, Resource Branch for Brain Disease Research, Center for Bioresource-Based Research, Brain Research Institute, [3]Department of Structural Pathology Institute of Nephrology, Graduate School of Medical and Dental Sciences, Niigata University, 1-757 Asahimachi, Niigata 951-8122, Japan and [4]Department of Neurology, Graduate School of Medicine, The University of Tokyo, 7-3-1 Hongo, Bunkyo-Ku, Tokyo113-8655, Japan

Received December 14, 2006; Revised March 1, 2007; Accepted March 1, 2007

ABSTRACT

Aprataxin is the causative gene product for early-onset ataxia with ocular motor apraxia and hypoalbuminemia/ataxia with oculomotor apraxia type 1 (EAOH/AOA1), the clinical symptoms of which are predominantly neurological. Although aprataxin has been suggested to be related to DNA single-strand break repair (SSBR), the physiological function of aprataxin remains to be elucidated. DNA single-strand breaks (SSBs) continually produced by endogenous reactive oxygen species or exogenous genotoxic agents, typically possess damaged 3′-ends including 3′-phosphate, 3′-phosphoglycolate, or 3′-α, β-unsaturated aldehyde ends. These damaged 3′-ends should be restored to 3′-hydroxyl ends for subsequent repair processes. Here we demonstrate by *in vitro* assay that recombinant human aprataxin specifically removes 3′-phosphoglycolate and 3′-phosphate ends at DNA 3′-ends, but not 3′-α, β-unsaturated aldehyde ends, and can act with DNA polymerase β and DNA ligase III to repair SSBs with these damaged 3′-ends. Furthermore, disease-associated mutant forms of aprataxin lack this removal activity. The findings indicate that aprataxin has an important role in SSBR, that is, it removes blocking molecules from 3′-ends, and that the accumulation of unrepaired SSBs with damaged 3′-ends underlies the pathogenesis of EAOH/AOA1. The findings will provide new insight into the mechanism underlying degeneration and DNA repair in neurons.

INTRODUCTION

Aprataxin is the causative gene product for early-onset ataxia with ocular motor apraxia and hypoalbuminemia, also called ataxia with oculomotor apraxia type 1 (EAOH/AOA1) (1,2), which is characterized by early-onset progressive ataxia, ocular motor apraxia, peripheral neuropathy and hypoalbuminemia (3–6). Aprataxin interacts with the X-ray repair cross-complementing group 1 protein (XRCC1) and poly(ADP-ribose) polymerase-1 (PARP-1), which are a scaffold protein and a molecular nick sensor in DNA single-strand break repair (SSBR), respectively (7–10), suggesting that aprataxin is associated with SSBR. Consistent with these observations, the lymphoblastoid cells from patients with EAOH/AOA1 show a high sensitivity to H_2O_2 and alkylating agents, which cause DNA single-strand breaks (SSBs) (11). In addition, aprataxin has the histidine triad (HIT) motif, which functions as nucleotidyl hydrolases (12–15), and the zinc finger motif, which is a DNA- or RNA-binding motif. These findings led to the hypothesis that aprataxin has catalytic activity in SSBR.

*To whom correspondence should be addressed. Tel: 81 25 227 0665; Fax: 81 25 223 6646; Email: onodera@bri.niigata-u.ac.jp

The authors wish it to be known that, in their opinion, the first two authors should be regarded as joint First Authors

SSBs are discontinuities in the sugar–phosphate backbone of one strand of a DNA duplex. In neurons, DNA is under continuous threat of damage by endogenous reactive oxygen species (ROS) or exogenous environmental genotoxins, and more than tens of thousands of SSBs arise in each cell per day (16). SSBs can arise directly from sugar damage, or indirectly from base damage via the enzymatic cleavage of the phosphodiester backbone as intermediate products of SSBR (16). The formation of another type of SSB is mediated by topoisomerase I (TOP1), which cleaves one strand of a DNA duplex during transcription or DNA replication (17,18). If SSBs are not repaired rapidly, they can cause transcription blockage or they are converted to lethal DNA double-strand breaks (DSBs), leading to cell dysfunction and cell death (19).

Most SSBs are accompanied by the loss of a single nucleotide; this loss must be filled by DNA polymerase and subsequently sealed by DNA ligase. DNA polymerase β (Pol β) and DNA ligase III (Lig3) are most commonly employed for gap filling and ligation during SSBR (8). SSBs arising directly from sugar damage or indirectly from base damage typically possess damaged 3′-ends: 3′-phosphate, 3′-phosphoglycolate (3′-PG), or 3′-α, β-unsaturated aldehyde ends. Because these damaged 3′-ends are not suitable for DNA polymerase or DNA ligase, enzymatic processing is required in SSBR to restore the damaged 3′-ends to suitable 3′-hydroxyl ends. 5′-Polynucleotide kinase 3′-phosphatase (PNKP) removes damaged 3′-phosphate ends, but not other damaged 3′-ends. Apurinic/apyrimidinic endonuclease (APE1) can remove 3′-phosphate, 3′-PG and 3′-α, β-unsaturated aldehyde ends (20). However, the 3′-PG and 3′-phosphate removal activities of APE1 are ~70-fold lower than the AP endonuclease activity of APE1 (21–23). Therefore, it is assumed that other enzymes can alternatively process these damaged 3′-ends.

In the present study, we hypothesized that aprataxin removes damaged 3′-ends and facilitates the repair of SSBs. Here we show that aprataxin has a novel removal activity with a unique substrate specificity toward damaged 3′-ends including 3′-PG and 3′-phosphate ends, and that disease-associated mutant forms of aprataxin lack this activity. The results indicate that aprataxin has an important and direct role in SSBR, that is, it removes blocking molecules from DNA 3′-ends, and that neurodegeneration in EAOH/AOA1 may be caused by the accumulation of unrepaired SSBs with damaged 3′-ends.

MATERIALS AND METHODS

Expression and purification of recombinant aprataxin

The long-form human aprataxin cDNA (GenBank accession number NM_175073) was amplified by polymerase chain reaction (PCR) using the primers 5′-CCGGATC CATGATGCGGGTGTGCTGGTTGG and 3′-GGCTC GAGTCACTGTGTCCAGTGCTTCCTG and the cDNA library (Human Ovary Marathon-Ready cDNA: Clonetech) as the template. The aprataxin cDNA fragment was inserted into the BamHI/XhoI site of the pFastBac™ donor plasmid, and this plasmid was transformed in DH10Bac™ competent cells to transpose into 'Bacmids' (Bac-to-Bac® Baculovirus Expression Systems, Invitrogen). Recombinant 'Bacmids' were purified using the High Purity Plasmid Miniprep System (Marligen), and infected to insect cells with the Cellfectin reagent according to the manufacturer's recommendation. A high-titer viral stock was obtained, and Sf9 cells were infected at a multiplicity of infection (MOI) of 10 for 72 h. Then, the cells were harvested and lysed in insect cell lysis buffer (BD Pharmingen) with 1× Complete Mini (Roche Diagnostic Corporation) for 30 min at 4°C. Recombinant human aprataxin was first purified by immobilized metal affinity chromatography (MagExtractor® His-tag protein purification kit, TOYOBO). The extracts were fractionated by gel filtration column chromatography (AKTA explorer 10S with HiLoad 16/60 Superdex 75 pg column, GE Healthcare) in 50 mM Tris-HCl (pH 7.5) and 100 mM NaCl. These fractionated extracts were desalinized using Slide-A-Lyzer® dialysis cassettes (Pierce Biotechnology), separated by denaturing sodium dodecyl sulfate-polyacrylamide gel electrophoresis (SDS-PAGE), and stained with Coomassie brilliant blue (CBB). Western blotting was performed using an anti-Tetra-His antibody (Quiagen) and an anti-aprataxin antibody (ab31841, Abcom).

Recombinant human Pol β, PNKP and Lig3 were expressed in silkworm *Bombyx mori* (Katakura). The cDNA fragment of each protein was amplified by PCR using the cDNA library (Human Ovary Marathon-Ready cDNA: Clontech) as the template and then inserted into pYNGHis (Katakura). The purified plasmid vector was mixed with purified cysteine proteinase-deleted viral DNA and then cotransfected in BmN cells of silkworm *Bombyx mori* larvae. The obtained recombinant virus was used for the infection of silkworm *Bombyx mori* pupae. Infected pupae were incubated at 25°C, and then frozen for 144 h postinoculation. Harvested pupae were lysed, and the His-tagged protein was purified by immobilized metal affinity chromatography (MagExtractor® His-tag protein purification kit, TOYOBO).

Mutant aprataxin cDNAs were produced using the GeneTailer site-directed mutagenesis system (Invitrogen). Wild-type long-form aprataxin (LA) cDNA, the forkhead-associated (FHA) domain of aprataxin (1–114 amino acids; FHA), the splicing variant of aprataxin (175–343 amino acids, GenBank accession number NP_7782411; SA) and the mutant forms of aprataxin cDNA fragments were inserted into the BamHI/XhoI site of pGEX-6P-3 (GE Healthcare Bio-Science Corp.). Glutathione S-transferase (GST) fusion proteins were overexpressed in Rosetta 2 (DE3) pLysS (Novagen) bacterial cells containing these plasmids. The bacterial cells were grown at 37°C until they reached an A_{600} of 1.0 and then induced with 1 mM isopropyl-1-thio-D-galactopyranoside and grown for another 3 h before harvesting. Cell pellets were lysed using BugBuster HT (Novagen) with EDTA-free complete protease inhibitor cocktail (Sigma). The GST-tagged proteins were purified using a GST fusion protein purification kit (Bulk GST Purification Modules®,

GE Healthcare). Purified fractions were desalinized using Slide-A-Lyzer® dialysis cassettes (Pierce Biotechnology), separated by denaturing SDS-PAGE, and stained with CBB. Western blotting was performed using an anti-GST antibody (GE Healthcare Bio-Science Corp.) and an anti-aprataxin antibody (ab31841, Abcom).

Oligonucleotide substrates

The sequences of DNA substrates used were as follows: FITC-21 (5′-[FITC]CTACGTCAGATCTGCGGATGT-3′), 21-OH (5′-CTACGTCAGATCTGCGGATGT[OH]-3′), 21-P (5′-CTACGTCAGATCTGCGGATGT[P]-3′), 24 (5′-CTCTAGCACTTGAGGCTATCCATG-3′), 23 (5′-TCTAGCACTTGAGGCTATCCATG-3′), 45 (5′-CATGGATAGCCTCAAGTGCTAGAGACATCCGC AGATCTGACGTAG-3′), FITC-21-PG (5′-[FITC]CTA CGTCAGATCTGCGGATGT-[PG]-3′), FITC-21-Y (5′-[FITC]CTACGTCAGATCTGCGGATGT-[Y]-3′), and 45/21(U) (5′-[FITC]CTACGTCAGATCTGCGGATGU CTCTAGCACTTGAGGCTATCCATG-3′). 5′-FITC-labeled oligonucleotides were synthesized and purified by high-performance liquid chromatography. A 5′-FITC-labeled 3′-PG 21-mer oligonucleotide (FITC-21-PG) was obtained from Thermo Electron Corporation. A 5′-FITC-labeled 3′-phosphotyrosine 21-mer oligonucleotide (FITC-21-Y) was purchased from Midland Certified Reagent Company. A 5′-FITC-labeled 21-mer oligonucleotide with 3′-phospho-α, β-unsaturated aldehyde was prepared using uracil DNA glycosylase (Invitrogen) and endonuclease III (BioLabs). To generate an apurinic/apyrimidinic (AP) site at the 21st uracil from 5′, 10 μM oligonucleotide FITC-45/21(U) was incubated with uracil DNA glycosylase (2 unit) for 1 h at 37°C in a mixture containing 20 mM Tris-HCl (pH 8.4), 10 mM $MgCl_2$ and 50 mM KCl. The reaction product was annealed with 10 μM oligonucleotide 45. Annealed oligonucleotides (2 μM) were treated with endonuclease III according to the manufacturer's instructions to generate the 5′-FITC-labeled 21-mer oligonucleotide with 3′-phospho-α, β-unsaturated aldehyde.

3′-End processing assay

To analyze the activity of aprataxin to remove 3′-phosphate, 1 pmol of oligonucleotides phosphorylated at the 3′-end was incubated in a mixture containing 100 mM Tris-HCl (pH 6.0), 10 mM $MgCl_2$, 10 mM β-ME and 0.1 mg/ml BSA with the indicated protein (25, 50 and 100 nM aprataxin, and 50 nM PNKP) for 1 h at 37°C. To analyze the activity of aprataxin to remove 3′-PG, 3′-phospho-α, β-unsaturated aldehyde or 3′-phosphotyrosine ends, 5′-FITC-labeled 21-mer oligonucleotides with 3′-PG, 3′-phospho-α, β-unsaturated aldehyde or 3′-phosphotyrosine ends were incubated with aprataxin (25, 50 and 100 nM), APE1 and TDP1 in a mixture containing 25 mM Tris-HCl (pH 7.5), 10 mM $MgCl_2$, 0.5 mM ATP, 0.1 mg/ml BSA and 1 mM DTT for 1 h at 37°C. Reactions were stopped by adding an equal volume of gel-loading buffer (80% formamide, 10 mM EDTA and 0.1% bromophenol blue). The products were separated by electrophoresis in a denaturing 20% polyacrylamide-8 M urea gel and visualized using a Typhoon 9400 scanner (GE Healthcare). We used APE1 (TREVIGEN) and TDP1 (Abnova Corporation) as the positive controls.

GMP- and AMP-lysine hydrolase assay

GMP- and AMP-lysine hydrolysis assay was performed using a method originally developed for FHIT with a fluorogenic substrate, GpppBODYPY (Molecular Probes) (15). We followed the protocol of this method previously described with a slight modification. Briefly, 100 μM GpppBODYPY or ApppBODYPY was incubated with the indicated amounts of recombinant proteins (His-LA, LA, SA and FHA) for 1 h at 37°C in 20 μl of 20 mM Na HEPES (pH 7.0), 0.5 mM $MnCl_2$ and 0.2 mg/ml BSA. Reactions were stopped by adding an equal volume of gel-loading buffer (80% formamide, 10 mM EDTA and 0.1% bromophenol blue). The products were separated by electrophoresis in a denaturing 20% polyacrylamide–8 M urea gel and visualized using a Typhoon 9400 scanner (GE Healthcare). We used Fhit (Upstate) as the positive control.

Preparation of DNA 5′-adenylates

DNA 5′-adenylate was essentially prepared as previously described (24). Briefly, a 12.5 μM 5′-phosphate 3′-FITC-labeled 24-mer oligonucleotide (P-24-FITC: 5′-[P]CTCTAGCACTTGAGGCTATCCATG[FITC]-3′) was annealed with a 25 μM 3′-phosphate 21-mer oligonucleotide (21-P: 5′-CTACGTCAGATCTGCGGATGT[P]-3′) and 25 μM complementary oligonucleotide 45. The annealed oligonucleotides were treated with 100 nM T4 DNA ligase in ligation buffer (50 mM Tris-HCl (pH7.5), 10 mM $MgCl_2$, 5 mM DTT, 25 μg/ml BSA and 1 mM ATP) overnight at 37°C. Because the nick cannot be ligated owing to 3′-end blocking with phosphate, the adenylation of the 5′-end occurs as an abortive ligation intermediate. The reaction product, 5′-AMP 3′-FITC-labeled 24-mer oligonucleotide (AMP-24-FITC), was then denatured and purified by separation on a denaturing 20% polyacrylamide–8 M urea gel. Following gel extraction, AMP-24-FITC was annealed with a 3′-hydroxyl 21-mer oligonucleotide (21-OH) and oligonucleotide 45.

DNA 5′-adenylate hydrolysis assay

DNA 5′-adenylate hydrolysis assay was performed as described previously with a slight modification (25). In brief, the 45-mer duplex DNA harboring a nick with 5′-adenylate ends was incubated with aprataxin or PNKP in a mixture containing 50 mM Tris-HCl (pH 7.5), 1 mM EDTA, 5 mM DTT for the indicated times at 37°C. Reactions were stopped by adding an equal volume of gel-loading buffer (80% formamide, 10 mM EDTA and 0.1% bromophenol blue). The products were separated and visualized as described above.

Reconstitution of SSBR

For the reconstitution of DNA repair, 5′-FITC-labeled 3′-phosphate 21-mer oligonucleotides (FITC-21-PO_3^-) were annealed with 45- and 23-mer oligonucleotides in

a mixture containing 1 mM $MgCl_2$, 20 mM Tris-HCl (pH 8.0) and 1 mM NaCl to form SSBs with 3′-end blocking with phosphate. The 5′-FITC-labeled 3′-hydroxyl oligonucleotide (FITC-21-OH) was used as the control of SSBs. For another DNA repair assay, FITC-21-PG oligonucleotides were annealed with 45- and 23-mer oligonucleotides to form SSBs with 3′-end blocking with PG. These substrates were incubated with Pol β, Lig3 and aprataxin for 90 min at 37°C. Reaction was stopped by adding an equal volume of gel-loading buffer. The products were separated by electrophoresis in a denaturing 20% polyacrylamide–8 M urea gel and visualized using a Typhoon 9400 scanner (GE Healthcare).

RESULTS

Aprataxin removes 3′-phosphate and 3′-phosphoglycolate ends

We constructed a histidine-tagged long-form human aprataxin (His-LA) using the baculovirus-protein-expression system (Figure 1A). His-LA was purified by a standard technique, followed by further purification by immobilized metal affinity and gel filtration column chromatography to remove any contamination by other proteins. A single band, which was reactive to the anti-aprataxin antibody, was observed by CBB staining for fractions from 14 to 19 (Figure 1C and E). The aprataxin-rich fraction (No. 15, Figure 1B–E) was used in the following studies.

To investigate the enzymatic activity of aprataxin against damaged 3′-ends, we examined the 3′-end processing activities of the recombinant aprataxin employing various 3′-end-modified oligonucleotides as substrates. When 3′-phosphate oligonucleotides were used as substrates, the 3′-phosphatase activity of aprataxin was clearly demonstrated by the mobility shift on a denaturing 20% polyacrylamide–8 M urea gel, in which 3′-phosphate oligonucleotides were electrophoresed faster than 3′-hydroxyl oligonucleotides (Figure 2A). By treating 3′-phosphate oligonucleotides with aprataxin, the bands corresponding to 3′-hydroxyl oligonucleotides appeared in a concentration-dependent manner (Figure 2A, lanes 3–5). Next, we determined whether aprataxin removes 3′-PG ends. Notably, as shown in Figure 2B, aprataxin removed 3′-PG ends and generated 3′-hydroxyl ends (Figure 2B). In contrast, aprataxin failed to remove 3′-α, β-unsaturated aldehyde or 3′-phosphotyrosine ends under the same conditions as those in which aprataxin removed 3′-phosphate or 3′-PG ends (Figure 2C and D). These results indicate that aprataxin has 3′-end processing activities toward 3′-phosphate and 3′-PG ends, but not toward 3′-α, β-unsaturated aldehyde or 3′-phosphotyrosine ends.

FHA domain of aprataxin and disease-associated mutant forms of aprataxin lack 3′-phosphatase and 3′-phosphoglycolate hydrolase activities

To confirm the 3′-phosphatase and 3′-PG hydrolase activities and determine the catalytic domain of aprataxin, we constructed five types of the aprataxin fusion protein including wild-type full-length aprataxin (long-form aprataxin, LA), two types of full-length mutant form of aprataxin (P206L and V263G), which are most frequently found in Japanese patients, the N-terminal FHA domain (FHA) of aprataxin, and aprataxin without the FHA domain (short-form aprataxin, SA) in the bacterial expression system (Figure 3A and B) (1). The GST-tagged long-form

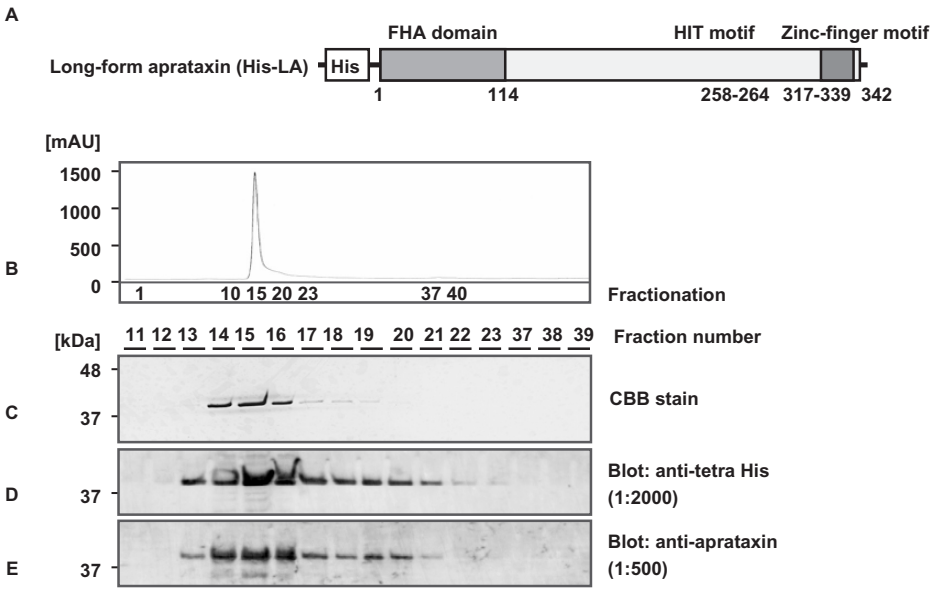

Figure 1. Expression and purification of recombinant aprataxin in baculovirus expression system. (**A**) Construct of His-tagged long-form aprataxin (His-LA) expressed using Bac-to-Bac® Baculovirus Expression System. (**B**) Chromatogram of gel-filtered aprataxin. Following immobilized metal affinity chromatography, the aprataxin-rich fraction was purified by gel filtration column chromatography. A major peak was observed for each of the fractions from 13 to 20 in the chromatogram. (**C**) The fractionated extracts were separated by SDS-PAGE and stained with Coomassie brilliant blue (CBB). A 39-kDa single band is detected for each of the fractions from 14 to 19. Western blot analysis using the anti-His antibody (**D**) and anti-aprataxin antibody (**E**) shows a 39-kDa immunoreactive product in each of the fractions from 13 to 21.

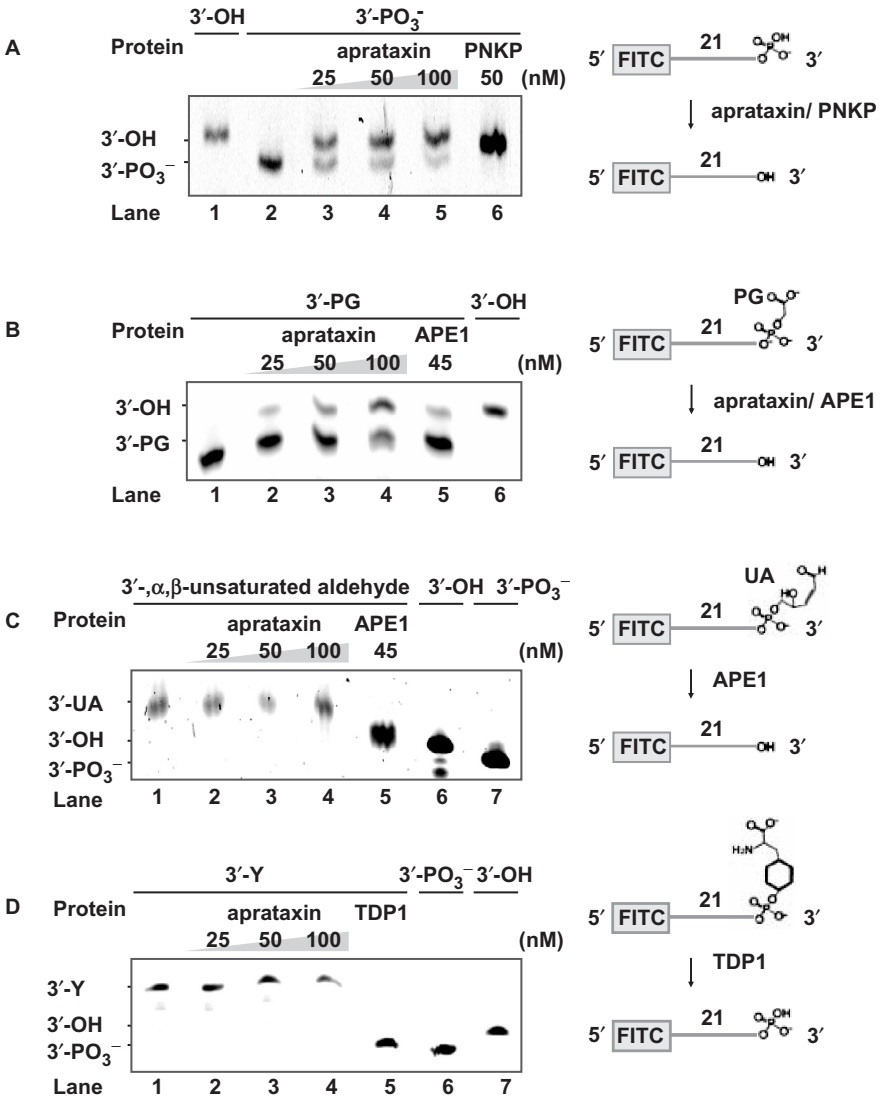

Figure 2. 3′-End processing by aprataxin. (**A**) Aprataxin removes 3′-phosphate. The 5′-FITC-labeled 3′-phosphate (3′-PO_3^-) oligonucleotide was incubated in the absence (lane 2) or presence of aprataxin at different concentrations (25, 50 and 100 nM, lanes 3–5). A band with the same size as that of the 3′-hydroxyl (3′-OH) oligonucleotide (lane 1) appears in lanes with aprataxin (lanes 3–5). 5′-Polynucleotide kinase 3′-phosphatase (PNKP) was used as the positive control (lane 6). Reaction products were separated by 20% PAGE and visualized using a fluorescence gel scanner. (**B**) Aprataxin removes DNA 3′-phosphoglycolate. The 5′-FITC–labeled 3′-phosphoglycolate (3′-PG) oligonucleotide was incubated in the absence (lane 1) or presence of aprataxin at different concentrations (25, 50 and 100 nM, lanes 2–4). The amount of the 3′-OH oligonucleotide increases with aprataxin concentration (lanes 2–4). Apurinic/apyrimidinic endonuclease (APE1) was used as the positive control (lane 5). (**C**) Aprataxin fails to remove 3′-α, β-unsaturated aldehyde. The 5′-FITC-labeled 3′-α, β-unsaturated aldehyde (3′-UA) oligonucleotide was incubated in the absence (lane 1) or presence of aprataxin at different concentrations (25, 50 and 100 nM, lanes 2–4). The amount of the 3′-UA oligonucleotide does not decrease with increasing aprataxin concentration (lanes 2–4). The 3′-OH oligonucleotides were generated in the presence of APE1 (lane 5). The faint smear corresponding to the 3′-UA oligonucleotide in lanes 1–5 is an artifact generated under the electrophoresis conditions employed. (**D**) Aprataxin fails to remove 3′-phosphotyrosine end. The 5′-FITC-labeled 3′-phosphotyrosine (3′-Y) oligonucleotide was incubated in the absence (lane 1) or presence of aprataxin at different concentrations (25, 50 and 100 nM, lanes 2–4). The amount of the 3′-Y oligonucleotide do not decrease with increasing aprataxin concentration (lanes 2–4). 3′-PO_3 oligonucleotides were generated in the presence of tyrosyl-DNA phosphodiesterase 1 (TDP1) (lane 5).

aprataxin (LA) showed 3′-phosphatase and 3′-PG hydrolase activities comparable to those of His-LA obtained from the baculovirus expression system (Figure 4A and B). Although SA removed 3′-phosphate and 3′-PG (Figure 4A and B), its removal activity was lower than that of LA. FHA did not show removal activity (Figure 4A and B).

Next, we examined whether mutant forms of aprataxin remove 3′-phosphate and 3′-PG ends. Although the mutant aprataxin proteins were unstable, we were able to produce full-length mutant forms of aprataxin (Figure 3B). These purified mutant proteins contained a ~63 kDa form, that is, full-length aprataxin and a ~46 kDa form that retained

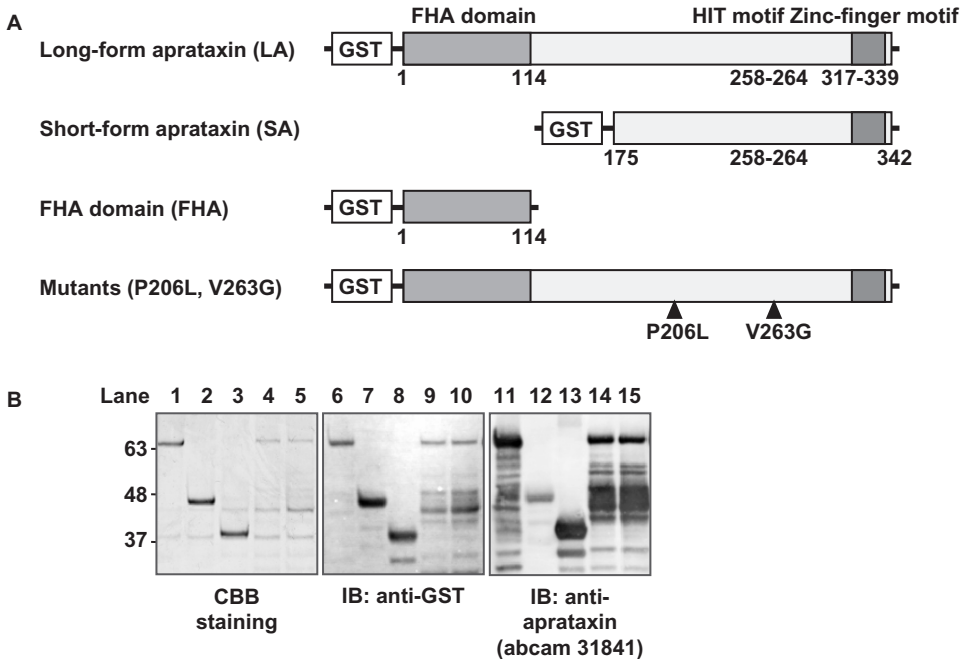

Figure 3. Expression of recombinant GST-aprataxin fusion protein. (**A**) Constructs of GST-aprataxin fusion proteins. Constructs of GST fusion protein containing full-length aprataxin (long-form aprataxin, LA), the C-terminal region of aprataxin (short-form aprataxin, SA), the N-terminal FHA domain of aprataxin (FHA) and full-length aprataxin with P206L or V263G (P206L, V263G). (**B**) Expression and purification of GST-aprataxin fusion proteins. Recombinant GST fusion proteins containing LA (lanes 1, 6 and 11), SA (lanes 2, 7 and 12), FHA (lanes 3, 8 and 13), P206L (lanes 4, 9 and 14) and V263G (lanes 5, 10 and 15) were expressed in the bacterial expression system. Purified products were analyzed by CBB staining (left panel), and western blotting using the anti-GST antibody (middle panel) or anti-aprataxin antibody (right panel).

NH_2-terminal GST. Neither P206L nor V263G removed 3′-phosphate or 3′-PG ends (Figure 4A and B).

The affinity and catalytic activity of these aprataxin proteins for these two substrates are shown in Table 1. LA showed the highest 3′-phosphatase and 3′-PG hydrolase activities, whereas SA showed the activities less than one-half of those of LA. FHA, P206L and V263G lacked the activities. These results indicate that the C-terminal region of aprataxin, which includes the HIT motif, is indispensable for these activities and the N-terminal region of 1–174 amino acids might enhance these activities.

We compared these activities of LA with those of PNKP or APE1 in parallel experiments. The turnover number (K_{cat}) of the 3′-phosphatase activity of LA was 10-fold lower than that of PNKP, whereas the K_{cat} of the 3′-phosphatase activity of PNKP under our conditions was lower than that previously reported (23) (Table 1). On the other hand, the K_{cat} of the 3′-PG hydrolase activity of LA was ~20-fold higher than that of APE1.

Substrate specificity of aprataxin

To investigate the substrate specificity of aprataxin, we compared the DNA 3′-phosphatase and 3′-PG hydrolase activities of aprataxin on single-stranded (ss) and double-stranded (ds) DNAs (Figure 5). The 3′-phosphatase activity of LA on recessed, gapped or nicked ds DNA is approximately one-half of that on ss DNA (Figure 5A–C). In contrast, the 3′-PG hydrolase activity of LA on both ss and gapped ds DNA with 3′-PG ends is 1.5-fold higher than that on recessed or nicked ds DNA (Figure 5D–F).

Aprataxin removes adenylate residues covalently linked to 5′-phosphate ends, and disease-associated mutant forms of aprataxin lack the activity

As aprataxin has been reported to have GMP- and AMP-lysine hydrolase activities, which are present in most proteins of the HIT superfamily (12–15), we investigated the GMP- and AMP-lysine hydrolase activities of aprataxin employing GpppBODIPY and ApppBODIPY as substrates. The full-length aprataxin fusion proteins His-LA and LA showed very low or no GMP- or AMP-lysine hydrolase activity at the same or a higher concentration used for the 3′-end processing assay (Figure 6A and B).

Recently, Ahel *et al.* have shown that aprataxin removes the adenylate residues on 5′-ends of SSBs via its hydrolase activity, thus resolving the abortive DNA ligation intermediates (25). Therefore, we investigated the 5′-adenylate monophosphate (AMP) removal activity of our GST-aprataxin fusion proteins. As similarly observed in their previous study (25), LA removed an adenylate residue from a 5′-end of nicked ds DNA (Figure 7A). In addition, SA showed a much lower 5′-AMP removal activity than LA, and FHA and disease-associated mutant forms (P206L and V263G) of aprataxin lacked the activity (Figure 7B and C).

Reconstitution of SSBR by recombinant human aprataxin, Pol β and Lig3

To confirm that the 3′-end processing activity of aprataxin is sufficient for SSBR by following the reactions carried out by Pol β and Lig3, we then reconstituted SSBR using

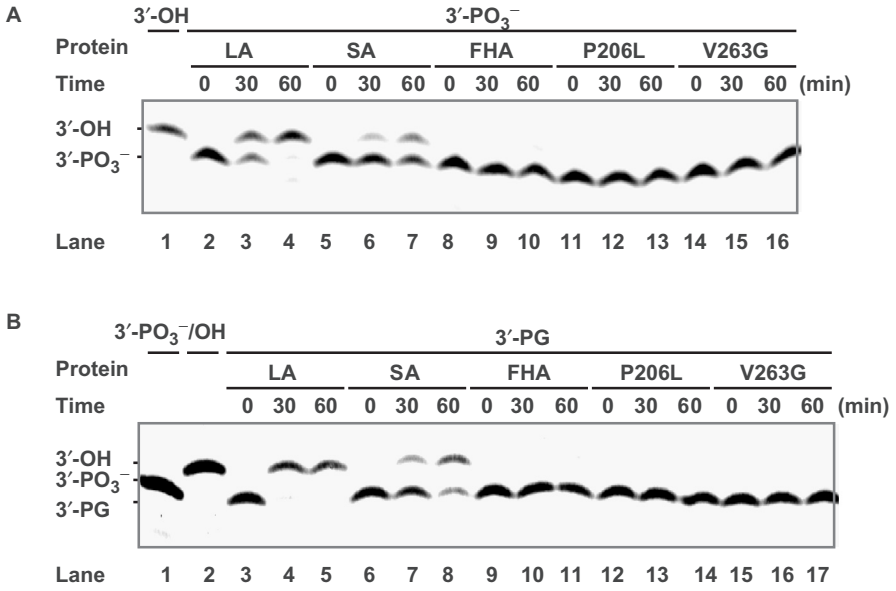

Figure 4. Disease-associated mutant forms of aprataxin lack their 3′-end processing activity. (**A**) Mutant forms of aprataxin fail to remove 3′-phosphate. The 5′-FITC-labeled 3′-phosphate (3′ - PO_3^-) oligonucleotide was incubated in the presence of 50 nM recombinant GST fusion proteins containing LA (lanes 2–4), SA (lanes 5–7), FHA (lanes 8–10), P206L (lanes 11–13), and V263G (lanes 14–16) at different incubation times (0, 30 and 60 min). A band of the same size as that corresponding to the 3′-hydroxyl (3′-OH) oligonucleotide (lane 1) appears in lanes with LA (lanes 3 and 4). SA showed a weak phosphatase activity (lanes 5–7). Neither FHA, P206L nor V263G showed phosphatase activity (lanes 8–16). (**B**) Mutant forms of aprataxin fail to remove 3′-phosphoglycolate. The 5′-FITC-labeled 3′-PG oligonucleotide was incubated in the presence of 50 nM recombinant GST fusion proteins containing LA (lanes 3–5), SA (lanes 6–8), FHA (lanes 9–11), P206L (lanes 12–14) and V263G (lanes 15–17) at different incubation times (0, 30 and 60 min). A band of the same size as that corresponding to the 3′-OH oligonucleotide (lane 2) appears in lanes with LA (lanes 3 and 4). SA showed a weak 3′-PG hydrolase activity (lanes 6–8). Neither FHA, P206L nor V263G removed 3′-PG (lanes 9–17).

Table 1. Enzymatic activity of recombinant forms of aprataxin determined using 3′-phosphate and 3′-phosphoglycolate oligonucleotides as substrates

	LA	SA	FHA	P206L	V263G	PNKP	APE1
3′-Phosphate							
K_{cat} (s^{-1})	0.00027 ± 0.00007	0.00015 ± 0.00001	<0.00002	<0.00002	<0.00002	0.00262 ± 0.00022	
K_m (nM)	129 ± 76	251 ± 58				228 ± 124	
3′-Phosphoglycolate							
K_{cat} (s^{-1})	0.00287 ± 0.00039	0.00160 ± 0.00009	<0.00002	<0.00002	<0.00002		0.00014 ± 0.00001
K_m (nM)	231 ± 37	292 ± 31					61 ± 28

GST fusion proteins containing full-length aprataxin (long-form aprataxin, LA), the C-terminal region of aprataxin (short-form aprataxin, SA), the N-terminal FHA domain of aprataxin (FHA), full-length aprataxin with P206L (P206L) and full-length aprataxin with V263G (V263G) were used.

gapped ds DNA with damaged 3′-ends as substrates. In this assay, aprataxin was assumed to restore damaged 3′-ends including 3′-phosphate and 3′-PG ends to 3′-hydroxyl ends that are suitable for Pol β and Lig3 (Figure 8A and B, right panel). First, we incubated the gapped ds DNA consisting of 3′-phosphate 21-mer oligonucleotides and 5′-phosphate 23-mer oligonucleotides annealed to complementary 45-mer oligonucleotides with Pol β and Lig3 in the presence or absence of His-LA. Here, 45-mer products were generated only in the presence of His-LA (Figure 8A, left panel). Next, we incubated gapped ds DNA consisting of 3′-PG 21-mer oligonucleotides and 5′-phosphate 23-mer oligonucleotides annealed to complementary 45-mer oligonucleotides with Pol β and Lig3 in the presence or absence of His-LA. As expected, 45-mer products were generated only in the presence of aprataxin (Figure 8B, left panel). These results clearly indicate that the 3′-phosphate and 3′-PG removal activities of aprataxin are sufficient for the 3′-end processing in reconstituted SSBR with Pol β and Lig3.

DISCUSSION

Here, we show that aprataxin specifically removes damaged 3′-ends including 3′-PG and 3′-phosphate ends. Through this action, aprataxin might act with DNA polymerase and ligase to repair SSBs with these damaged 3′-ends. In addition, the C-terminal region of aprataxin is responsible for the removal activity and the region of 1–174 amino acids of aprataxin might enhance the

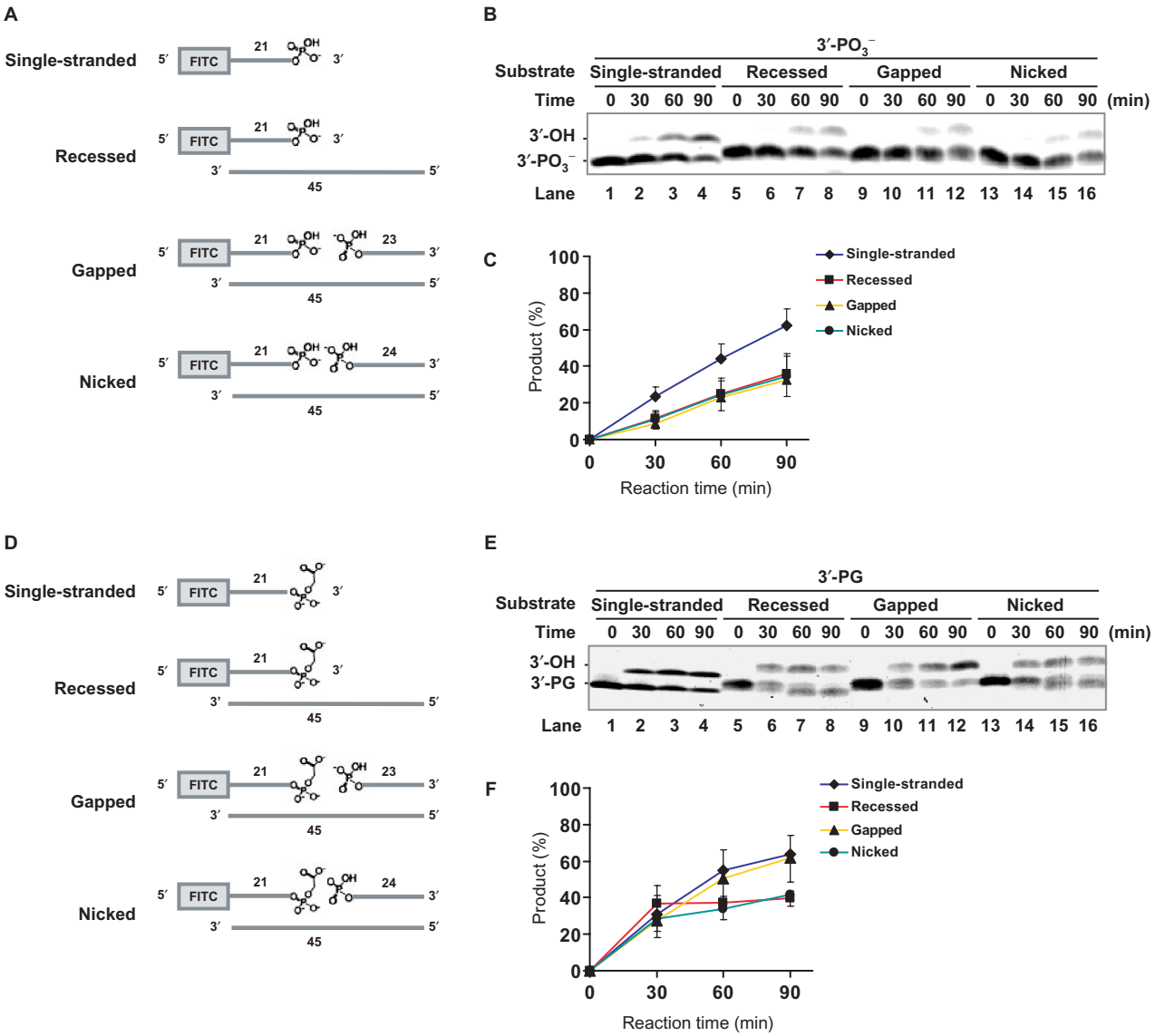

Figure 5. Aprataxin 3′-end processing activities on ss and ds DNA substrates. (**A–C**) 3′-Phosphatase activity of aprataxin on ss and ds DNA substrates. (A) The ss, recessed, one-nucleotide gapped and nicked DNA substrates with 3′-phosphate ends used are shown schematically. (B) Aprataxin preferentially acts on ss DNA. The substrates were incubated with 20 nM LA for the indicated times (0, 30, 60 and 90 min) at 37°C. Products were separated by denaturing PAGE and visualized using a Typhoon 9400 scanner (GE Healthcare). (C) Production rates in each reaction were quantified by ImageQuant TL (GE Healthcare). Error bars indicate standard errors for more than three independent experiments. (**D–F**) 3′-PG hydrolase activity of aprataxin on ss and ds DNA substrates. (D) The ss, recessed, one-nucleotide gapped and nicked DNA substrates with 3′-PG ends used are shown schematically. (E) Aprataxin preferentially acts on ss and gapped DNA. The substrates were incubated with 20 nM LA for the indicated times (0, 30, 60 and 90 min) at 37°C. (F) Production rates in each reaction were quantified as described above.

removal activity. Furthermore, the disease-associated mutant forms of aprataxin P206L and V263G lack the removal activity, strongly suggesting that the loss of the removal activity of aprataxin is closely linked to the pathogenesis of EAOH/AOA1.

The removal of damaged 3′-ends is important for repairing SSBs. SSBs arising directly from sugar damage usually possess 3′-phosphate or 3′-PG ends, whereas SSBs arising indirectly from base damage, via the enzymatic cleavage of the DNA backbone, possess 3′-α, β-unsaturated aldehyde, or 3′-phosphate ends (16,26). The formation of another type of SSB is mediated by TOP1, which cleaves one strand of a ds DNA during transcription or DNA replication and covalently binds at the 3′-ends with the tyrosyl-DNA phosphodiester linkage (17) (Figure 9). Several enzymes including a multiprotein complex with XRCC1 have been proposed as candidates for removing these damaged 3′-ends. PNKP might restore damaged 3′-phosphate ends, but not other damaged 3′-ends (23,27). APE1 is assumed to remove damaged 3′-phosphate, 3′-PG or 3′-α, β-unsaturated aldehyde ends; however, its enzymatic activity for removing 3′-phosphate or 3′-PG is extremely

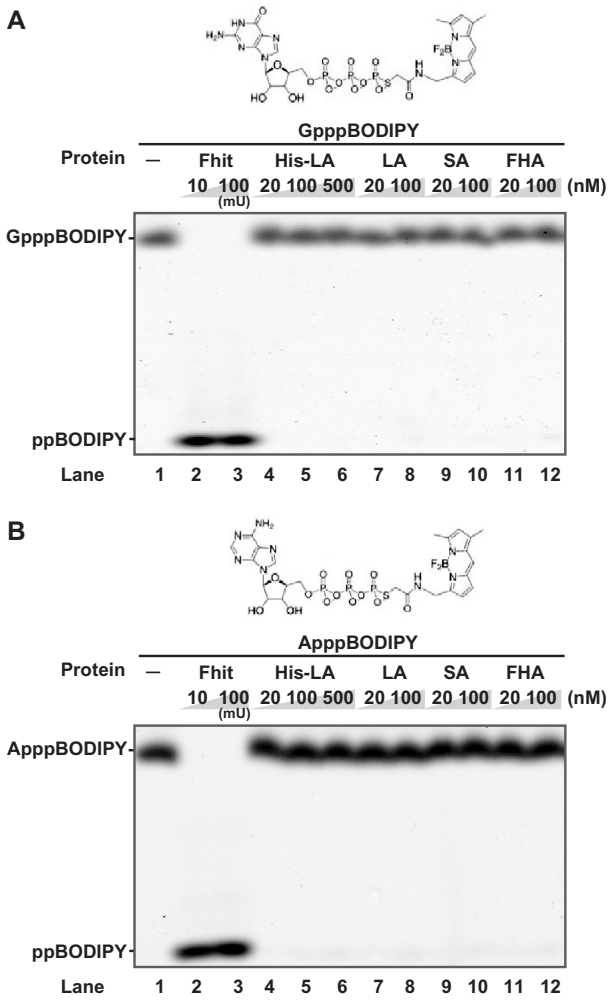

Figure 6. Recombinant aprataxin fails to efficiently hydrolase GpppBODIPY or ApppBODIPY. GpppBODIPY (**A**) or ApppBODIPY (**B**) was incubated with recombinant His-tagged long-form aprataxin obtained from the baculovirus expression system (His-LA, lanes 4–6), recombinant GST fusion proteins containing LA (lanes 7 and 8), SA (lanes 9 and 10) and FHA (lanes 11 and 12). None of them showed lysine hydrolase activity (lanes 4–12). Fhit at 10 and 100 mU as the positive control showed GMP-lysine hydrolase activity (lanes 2 and 3).

lower than its AP endonuclease activity (21–23). The results using fusion proteins expressed in baculovirus and bacterial expression systems clearly showed that aprataxin restores the damaged 3′-PG and 3′-phosphate ends to 3′-hydroxyl ends, but not 3′-α, β-unsaturated aldehyde ends nor phosphotyrosine ends. Moreover, the 3′-PG removal activity of aprataxin is higher than that of APE1 and prefers the gapped ds DNA as well as ss DNA, although the 3′-phosphate removal activity of aprataxin is lower than that of PNKP and prefers the ss DNA, not ds DNA. The results suggest that aprataxin is associated with the removal of damaged 3′-ends, particularly 3′-PG ends, directly induced by sugar damage, whereas APE1 is associated with the removal of damaged 3′-α, β-unsaturated aldehyde ends induced by base damage as well as the endonucleolytic cleavage of an AP site (Figure 9A and B). By contrast, although both PNKP and aprataxin might restore damaged 3′-phospohate ends, (Figure 9B and C), these proteins are found in mutually exclusive complexes with XRCC1 (28); therefore, they might function independently of each other in the repair of SSBs induced by sugar damage (Figure 9B and C). The precise physiological roles of PNKP and aprataxin in SSBR, however, await further investigations.

In DNA ligation, DNA ligase transfers AMP residues to 5′-ends of the DNA breaks and catalyzes the displacement of the adenylate residues on 5′-ends by attacking the adjacent 3′-hydroxyl group. When 3′-ends are damaged and non-ligated, the adenylate residues remain on 5′-ends of SSBs as abortive DNA-ligation intermediates. Recently, Ahel *et al*. have shown that aprataxin removes the adenylate residues on 5′-ends of SSBs (25). As reported in their article (25), aprataxin used in the present study also removed an adenylate residue from a 5′-end of nicked ds DNA. These results indicate that aprataxin contributes to processing the 'dirty ends', both 3′- and 5′-ends, of the DNA breaks. Furthermore, the disease-associated mutant forms of aprataxin lost their 3′- and 5′-end processing activities, suggesting the importance of the activities for EAOH/AOA1 pathogenesis. To determine the main physiological role of aprataxin in SSBR, we have to show the accumulation of SSBs with these dirty ends in tissues from patients with EAOH/AOA1 in future studies.

The clinical phenotype of EAOH/AOA1 is specifically restricted to the nervous system, raising the possibility that the activity of aprataxin to remove 3′-phosphate or 3′-PG ends plays an important role in neurons. Tyrosyl-DNA phosphodiesterase 1 (TDP1), the causative gene product for spinocerebellar ataxia with axonal neuropathy type 1 (SCAN1), removes the TOP1 peptide from 3′-ends in SSBs induced by TOP1. In addition to its tyrosyl-DNA phosphodiesterase activity, TDP1 has been also proposed to remove 3′-PG ends and function in the repair of SSBs induced by oxidative stress (17,29). The clinical phenotype of SCAN1 is similar to that of EAOH/AOA1, because they include cerebellar degeneration, posterior column involvement and peripheral axonal neuropathy without predisposition to malignancy (30). These similarities between EAOH/AOA1 and SCAN1 suggest that the removal of damaged 3′-ends, particularly those induced by oxidative stress, is crucial for the viability and function of neurons, in particular Purkinje cells and dorsal root ganglion cells.

The unique properties of neurons including a high rate of ROS production and a high transcriptional activity may lead to the generation of more SSBs compared with non-neuronal cells. Furthermore, although mitotic cells can utilize a homologous recombination machinery to compensate for a defect in SSBR, postmitotic neurons are unable to repair damaged DNA molecules in a DNA-replication-dependent manner and they are highly dependent on SSBR for DNA integrity. Therefore, neurons might be vulnerable to a defect in SSBR. The reason why a specific neuronal subtype is vulnerable to impairment of the aprataxin-dependent or TDP1-dependent SSBR system remains to be elucidated. Further studies on the

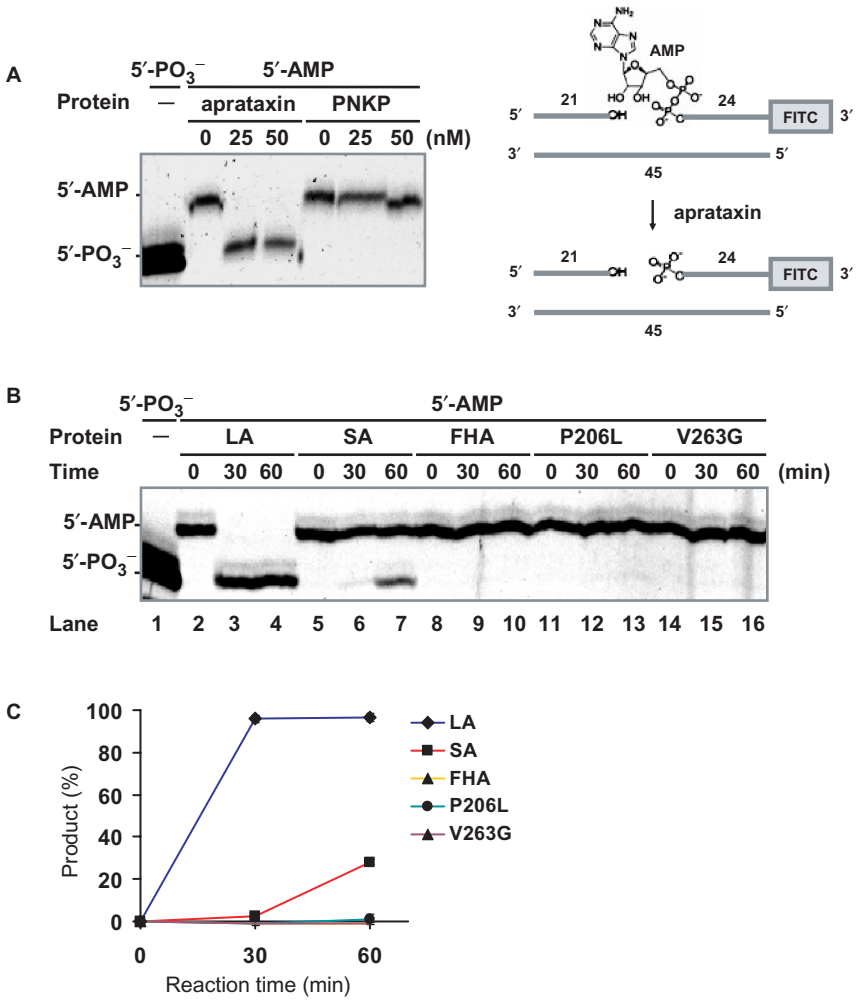

Figure 7. Removal of adenylate residues from 5′-ends by aprataxin. (**A**) Aprataxin removes AMP from 5′-ends of nicked ds DNA. The 45-mer ds DNA harboring a nick with 5′-AMP ends was incubated with the indicated amounts of aprataxin for 1 h. A band of the same size as that corresponding to the 5′-phosphate (5′ - PO_3^-) oligonucleotide appears in lanes with aprataxin. PNKP was used as the negative control. (**B**) Mutant forms of aprataxin fail to remove 5′-AMP. The 45-mer ds DNA harboring a nick with 5′-AMP ends was incubated in the presence of 50 nM recombinant GST fusion proteins containing LA (lanes 2–4), SA (lanes 5–7), FHA (lanes 8–10), P206L (lanes 11–13) and V263G (lanes 14–16) at different incubation times (0, 30 and 60 min). SA showed a lower 5′-AMP hydrolysis activity (lanes 5–7) than LA. Neither FHA, P206L nor V263G removed 5′-AMP (lanes 8–16). (**C**) Production rates in each reaction were quantified. Error bars indicate standard errors for more than three independent experiments.

mechanism underlying neuronal death and dysfunction caused by a defect in SSBR should provide new insights into therapeutic approaches for neurodegenerative disorders.

SUPPLEMENTARY DATA

Supplementary Data is available at NAR online.

ACKNOWLEDGEMENTS

This study was supported in part by a Grant-in-Aid for Scientific Research on Priority Areas 'Advanced Brain Science Project' and 'Applied Genomics', a Grant-in-Aid for Scientific Research (A) and (B) from the Ministry of Education, Culture, Sports, Science and Technology of Japan, a grant for the Research for the Future Program from the Japan Society for the Promotion of Science, a grant for 'the Research Committee for Ataxic Diseases' of the Research on Measures for Intractable Diseases from the Ministry of Health, Labor and Welfare, Japan, a grant from the Virtual Research Institute of Aging of Nippon Boehringer Ingelheim, a grant from the Naito Foundation, and grants from the Takeda Science Foundation, Suzuken Memorial Foundation, and Tsubaki Memorial Neuroscience Research Foundation. 'the Research Committee for Ataxic Diseases' of the Research on Measures for Intractable Diseases from the Ministry of Health, Welfare and Labour, Japan. Funding to pay the Open Access publication charge was provided by A Grant-in-Aid for Scientific Research on Priority Areas "Applied Genomics".

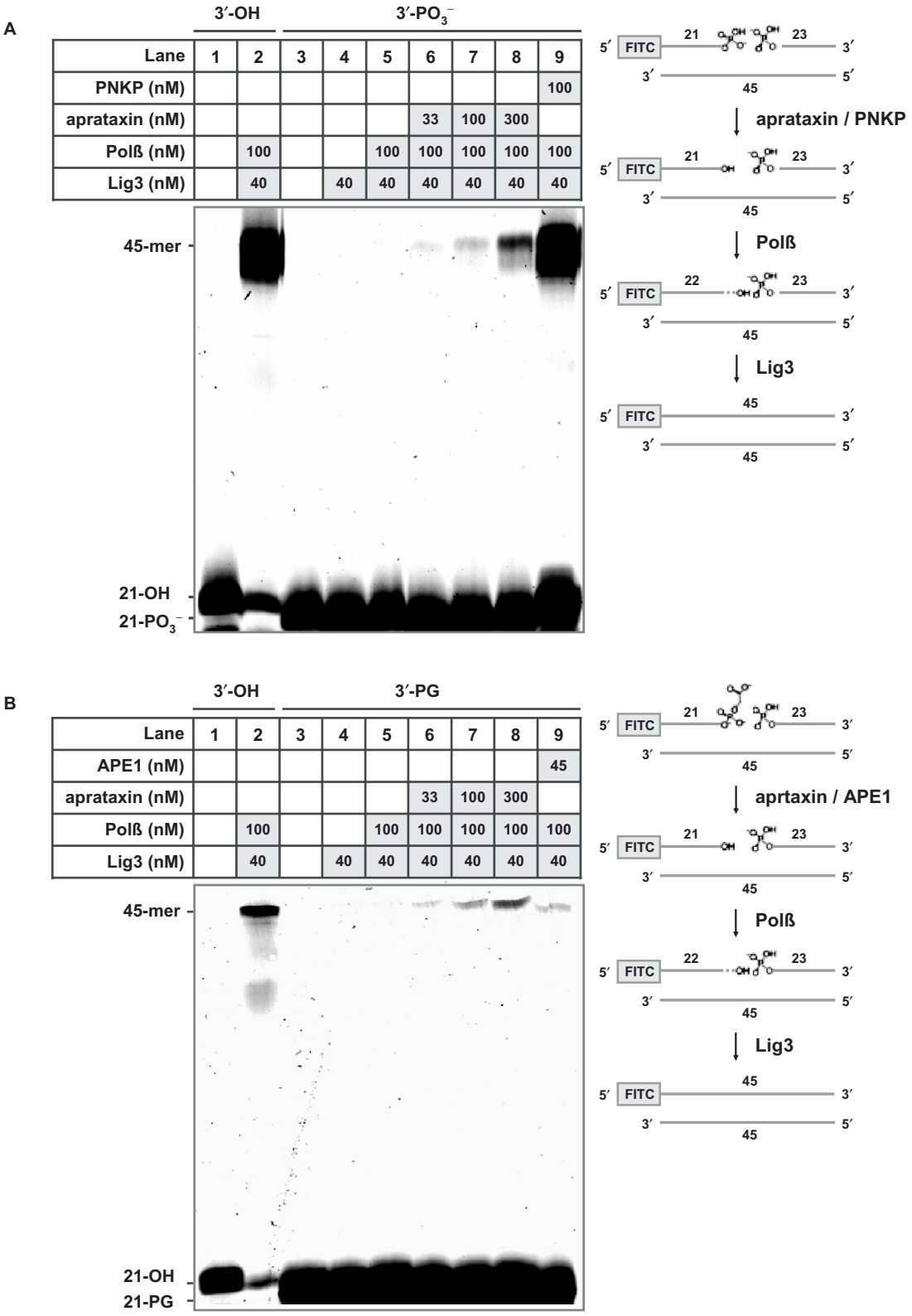

Figure 8. Aprataxin repairs SSBs with damaged 3′-ends. (**A**) DNA repair assay employing gapped dsDNA with 3′-phosphate ends as substrate. The 45-mer ds DNA substrate harboring a 1-nt gap with 3′-phosphate (3′ - PO_3^-) ends was incubated in the absence (lane 3) or presence of each of the indicated recombinant human proteins for 90 min (lanes 4–9). The 45-mer ds DNA substrate, harboring a 1-nt gap with 3′-hydroxyl (3′-OH) ends, was incubated in the absence (lane 1) or presence of each indicated recombinant human protein (lane 2). Complete repair is indicated by the generation of the 5′-FITC-labeled 45-mer oligonucleotide. The amount of 5′-FITC-labeled 45-mer increased with the concentration of aprataxin (lanes 6–8). PNKP was used as the positive control (lane 9). (**B**) DNA repair assay employing gapped dsDNA with 3′-phosphoglycolate ends as substrate. The 45-mer duplex substrate harboring a 1-nt gap with 3′-phosphoglycolate (3′-PG) ends was incubated in the absence (lane 3) or presence of each of the indicated recombinant human proteins for 90 min (lanes 4–9). The 45-mer duplex substrate harboring a 1-nt gap with 3′-OH ends was incubated in the absence (lane 1) or presence of each indicated recombinant human protein (lane 2). The amount of the FITC-labeled 45-mer oligonucleotide increases with aprataxin concentration (lanes 6–8). APE1 was used as the positive control (lane 9). The structures of the substrates employed in these experiments are shown on the right side of each panel.

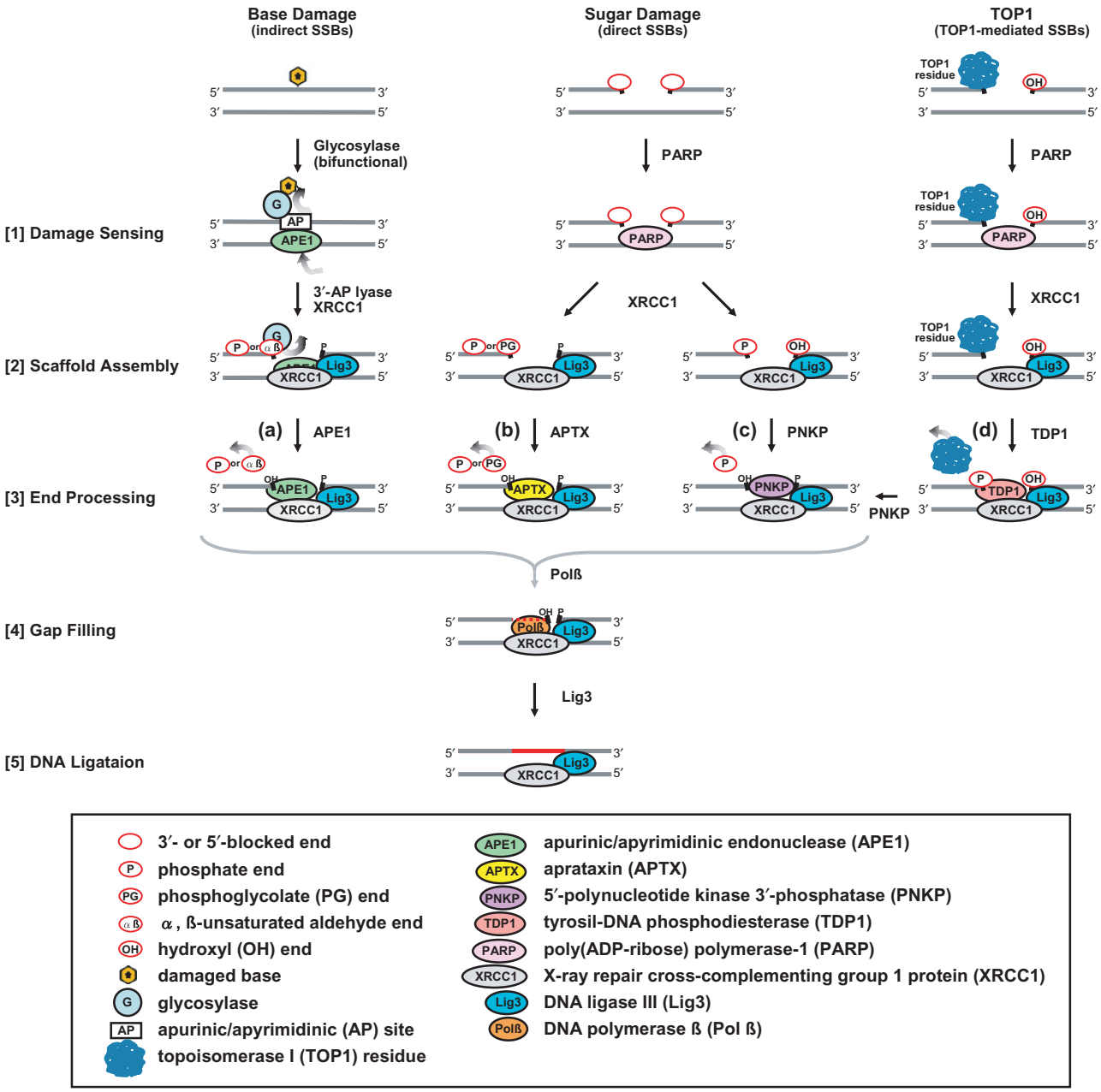

Figure 9. Model of aprataxin-dependent SSBR pathway. Four SSBR pathways defined by the type of enzyme that removes damaged 3′-ends are shown (a, b, c and d). SSBs can arise directly from sugar damage or TOP1 cleavage or indirectly from base damage. Red circles denote the damaged ends, the specific types of which are dependent on the source of the break. [1,2] PARP detects SSBs, thereby recruiting the XRCC1 and Lig3 complex. XRCC1 then replaces PARP. [**3**] The processing of damaged 3′-ends is mediated by either APE1 (**a**), aprataxin (**b**), PNKP (**c**) or TDP1 (**d**), depending on the type of damaged 3′-end. These damaged 3′-ends should be converted to 3′-OH ends for subsequent repair processes. In the pathway for repairing indirectly induced SSBs, damaged 3′-α, β unsaturated aldehyde ends are removed by APE1 (a). In the pathway for repairing directly induced SSBs, 3′-PG ends might be removed by aprataxin (b) and 3′-phosphate ends by aprataxin or PNKP (b,c). In the pathway for repairing TOP1-mediated SSBs, TOP1 covalent complexes at the 3′-ends are restored to 3′-phosphate ends by TDP1 (d). [**4**] After removing damaged 3′-ends, Pol β fills the gap (red dot line). [**5**] Lig3 seals the single-strand nick (red line).

Conflict of interest statement. None declared.

REFERENCES

1. Date,H., Onodera,O., Tanaka,H., Iwabuchi,K., Uekawa,K., Igarashi,S., Koike,R., Hiroi,T., Yuasa,T. *et al.* (2001) Early-onset ataxia with ocular motor apraxia and hypoalbuminemia is caused by mutations in a new HIT superfamily gene. *Nat. Genet.*, **29**, 184–188.
2. Moreira,M.C., Barbot,C., Tachi,N., Kozuka,N., Uchida,E., Gibson,T., Mendonca,P., Costa,M., Barros,J. *et al.* (2001) The gene mutated in ataxia-ocular apraxia 1 encodes the new HIT/Zn-finger protein aprataxin. *Nat. Genet.*, **29**, 189–193.
3. Fukuhara,N., Nakajima,T., Sakajiri,K., Matsubara,N. and Fujita,M. (1995) Hereditary motor and sensory neuropathy associated with cerebellar atrophy (HMSNCA): a new disease. *J. Neurol. Sci.*, **133**, 140–151.

4. Aicardi,J., Barbosa,C., Andermann,E., Andermann,F., Morcos,R., Ghanem,Q., Fukuyama,Y., Awaya,Y. and Moe,P. (1988) Ataxia-ocular motor apraxia: a syndrome mimicking ataxia-telangiectasia. *Ann. Neurol.*, **24**, 497–502.
5. Barbot,C., Coutinho,P., Chorao,R., Ferreira,C., Barros,J., Fineza,I., Dias,K., Monteiro,J., Guimaraes,A. *et al.* (2001) Recessive ataxia with ocular apraxia: review of 22 Portuguese patients. *Arch. Neurol.*, **58**, 201–205.
6. Sekijima,Y., Ohara,S., Nakagawa,S., Tabata,K., Yoshida,K., Ishigame,H., Shimizu,Y. and Yanagisawa,N. (1998) Hereditary motor and sensory neuropathy associated with cerebellar atrophy (HMSNCA): clinical and neuropathological features of a Japanese family. *J. Neurol. Sci.*, **158**, 30–37.
7. Date,H., Igarashi,S., Sano,Y., Takahashi,T., Takano,H., Tsuji,S., Nishizawa,M. and Onodera,O. (2004) The FHA domain of aprataxin interacts with the C-terminal region of XRCC1. *Biochem. Biophys. Res. Commun.*, **325**, 1279–1285.
8. Caldecott,K.W. (2003) XRCC1 and DNA strand break repair. *DNA Repair (Amst.)*, **2**, 955–969.
9. Clements,P.M., Breslin,C., Deeks,E.D., Byrd,P.J., Ju,L., Bieganowski,P., Brenner,C., Moreira,M.C., Taylor,A.M. *et al.* (2004) The ataxia-oculomotor apraxia 1 gene product has a role distinct from ATM and interacts with the DNA strand break repair proteins XRCC1 and XRCC4. *DNA Repair (Amst.)*, **3**, 1493–1502.
10. Sano,Y., Date,H., Igarashi,S., Onodera,O., Oyake,M., Takahashi,T., Hayashi,S., Morimatsu,M., Takahashi,H. *et al.* (2004) Aprataxin, the causative protein for EAOH is a nuclear protein with a potential role as a DNA repair protein. *Ann. Neurol.*, **55**, 241–249.
11. Gueven,N., Becherel,O.J., Kijas,A.W., Chen,P., Howe,O., Rudolph,J.H., Gatti,R., Date,H., Onodera,O. *et al.* (2004) Aprataxin, a novel protein that protects against genotoxic stress. *Hum. Mol. Genet.*, **13**, 1081–1093.
12. Hirano,M., Furiya,Y., Kariya,S., Nishiwaki,T. and Ueno,S. (2004) Loss of function mechanism in aprataxin-related early-onset ataxia. *Biochem. Biophys. Res. Commun.*, **322**, 380–386.
13. Seidle,H.F., Bieganowski,P. and Brenner,C. (2005) Disease-associated mutations inactivate AMP-lysine hydrolase activity of Aprataxin. *J. Biol. Chem.*, **280**, 20927–20931.
14. Kijas,A.W., Harris,J.L., Harris,J.M. and Lavin,M.F. (2006) Aprataxin forms a discrete branch in the HIT (histidine triad) superfamily of proteins with both DNA/RNA binding and nucleotide hydrolase activities. *J. Biol. Chem.*, **281**, 13939–13948.
15. Draganescu,A., Hodawadekar,S.C., Gee,K.R. and Brenner,C. (2000) Fhit-nucleotide specificity probed with novel fluorescent and fluorogenic substrates. *J. Biol. Chem.*, **275**, 4555–4560.
16. Caldecott,K.W. (2001) Mammalian DNA single-strand break repair: an X-ra(y)ted affair. *Bioessays*, **23**, 447–455.
17. El-Khamisy,S.F., Saifi,G.M., Weinfeld,M., Johansson,F., Helleday,T., Lupski,J.R. and Caldecott,K.W. (2005) Defective DNA single-strand break repair in spinocerebellar ataxia with axonal neuropathy-1. *Nature*, **434**, 108–113.
18. Leppard,J.B. and Champoux,J.J. (2005) Human DNA topoisomerase I: relaxation, roles, and damage control. *Chromosoma*, **114**, 75–85.
19. Caldecott,K.W. (2004) DNA single-strand breaks and neurodegeneration. *DNA Repair (Amst.)*, **3**, 875–882.
20. Parsons,J.L., Dianova,I.I. and Dianov,G.L. (2004) APE1 is the major 3′-phosphoglycolate activity in human cell extracts. *Nucleic Acids Res.*, **32**, 3531–3536.
21. Winters,T.A., Henner,W.D., Russell,P.S., McCullough,A. and Jorgensen,T.J. (1994) Removal of 3′-phosphoglycolate from DNA strand-break damage in an oligonucleotide substrate by recombinant human apurinic/apyrimidinic endonuclease 1. *Nucleic Acids Res.*, **22**, 1866–1873.
22. Suh,D., Wilson,D.M.III and Povirk,L.F. (1997) 3′-Phosphodiesterase activity of human apurinic/apyrimidinic endonuclease at DNA double-strand break ends. *Nucleic Acids Res.*, **25**, 2495–2500.
23. Wiederhold,L., Leppard,J.B., Kedar,P., Karimi-Busheri,F., Rasouli-Nia,A., Weinfeld,M., Tomkinson,A.E., Izumi,T., Prasad,R. *et al.* (2004) AP endonuclease-independent DNA base excision repair in human cells. *Mol. Cell*, **15**, 209–220.
24. Chiuman,W. and Li,Y. (2002) Making AppDNA using T4 DNA ligase. *Bioorg. Chem.*, **30**, 332–349.
25. Ahel,I., Rass,U., El-Khamisy,S.F., Katyal,S., Clements,P.M., McKinnon,P.J., Caldecott,K.W. and West,S.C. (2006) The neurodegenerative disease protein aprataxin resolves abortive DNA ligation intermediates. *Nature*, **443**, 713–716.
26. Sugimoto,T., Igawa,E., Tanihigashi,H., Matsubara,M., Ide,H. and Ikeda,S. (2005) Roles of base excision repair enzymes Nth1p and Apn2p from *Schizosaccharomyces pombe* in processing alkylation and oxidative DNA damage. *DNA Repair (Amst.)*, **4**, 1270–1280.
27. Inamdar,K.V., Pouliot,J.J., Zhou,T., Lees-Miller,S.P., Rasouli-Nia,A. and Povirk,L.F. (2002) Conversion of phosphoglycolate to phosphate termini on 3′ overhangs of DNA double strand breaks by the human tyrosyl-DNA phosphodiesterase hTdp1. *J. Biol. Chem.*, **277**, 27162–27168.
28. Luo,H., Chan,D.W., Yang,T., Rodriguez,M., Chen,B.P., Leng,M., Mu,J.J., Chen,D., Songyang,Z. *et al.* (2004) A new XRCC1-containing complex and its role in cellular survival of methyl methanesulfonate treatment. *Mol. Cell. Biol.*, **24**, 8356–8365.
29. Zhou,T., Lee,J.W., Tatavarthi,H., Lupski,J.R., Valerie,K. and Povirk,L.F. (2005) Deficiency in 3′-phosphoglycolate processing in human cells with a hereditary mutation in tyrosyl-DNA phosphodiesterase (TDP1). *Nucleic Acids Res.*, **33**, 289–297.
30. Takashima,H., Boerkoel,C.F., John,J., Saifi,G.M., Salih,M.A., Armstrong,D., Mao,Y., Quiocho,F.A., Roa,B.B. *et al.* (2002) Mutation of TDP1, encoding a topoisomerase I-dependent DNA damage repair enzyme, in spinocerebellar ataxia with axonal neuropathy. *Nat. Genet.*, **32**, 267–272.